

On the Electrooxidation and Amperometric Detection of NO Gas at the Pt/Nafion® Electrode

Kuo-Chuan Ho*, Wen-Tung Hung and Jin-Cherng Yang

Department of Chemical Engineering, National Taiwan University, Taipei, Taiwan 10617, R. O. C.

Tel. (+886) 2-2366-0739, Fax (+886) 2-2362-3040, e-mail: kcho@ms.cc.ntu.edu.tw

* Author to whom correspondence should be addressed.

Received: 22 May 2003 / Accepted: 03 June 2003 / Published: 22 August 2003

Abstract: The electrochemical oxidation of nitric oxide (NO) gas at the Pt/Nafion® electrode has been studied at a concentration of 500 ppm. The electrooxidation of NO taking place over a wide potential range can be described by a transcendental equation, from which the half-wave potential of the reaction can be determined. For NO oxidation with appreciable overpotentials but negligible mass-transfer effects, the Tafel kinetics applies. The obtained charge transfer coefficient (α) and the exchange current density (i_o) are 0.77 and 14 $\mu\text{A}/\text{cm}^2$, respectively. An amperometric NO gas sensor based on the Pt/Nafion® electrode has been fabricated and tested over the NO concentration range from 0 to 500 ppm. The Pt/Nafion® electrode was used as an anode at a fixed potential, preferably 1.15 V (vs. Ag/AgCl/sat. KCl), which assures current limitation by diffusion only. The sensitivity of the electrochemical sensor was found to be 1.86 $\mu\text{A}/\text{ppm}/\text{cm}^2$. The potential interference by other gases, such as nitrogen dioxide (NO₂) and carbon monoxide (CO), was also studied in the range 0–500 ppm. Both sensitivity for NO and selectivity of NO over NO₂/CO show significant enhancement upon using a cyclic voltammetric (CV) activation, or cleaning procedure.

Keywords: Amperometric sensor, Interference gas, Nitric oxide (NO), Pt/Nafion® electrode, Sensitivity.

Introduction

Nitric oxide (NO) gas, which is released from automobiles and combustion facilities, is a toxic gas. It also causes photochemical smog and acid rain. Monitoring of NO in gas pollutant has become an important task for the protection of global environments.

The NO also plays a functional role in the biological central nervous system and there exist an extensive literature on the determination of NO in the liquid. Most measurements of NO release in the biological solutions have involved indirect methods based on chemical detection of the oxidation products removed from biological system. Other bioassays have been proposed based on the physiological effects of NO such as the relaxation of blood vessels, stimulation of guanylated cyclase or the inhibition of platelet aggregation. Electrochemical (or amperometric) detection of NO in the aqueous phase generally has been accepted as the most reliable and sensitive technique available. A variety of sensing electrode, usually made of platinum and carbon electrodes or their composites, is mainly used for amperometric NO liquid sensing, for example, in the phosphate buffer solution. The electrodes employed include Pt/Nafion® [1-2], Pt/Nafion®/cellulose acetate [1], Pt/Ir [3], Pt/poly(4,4'-DHB) [4], C/NiP/Nafion® [5-6], C/Nafion® [2,7-9], C/silicon [10], and M(salen)/Nafion® [11]. Table 1 summarizes the operating condition, NO concentration range, and detection limit in the solution phase studied on various sensing electrodes.

The concentration of NO gas is generally measured using chemiluminescence (by the reaction of O₃ and NO) and electrochemical methods. The advantages of the electrochemical method are quicker response and lower cost compared to the chemiluminescence method. Two types of NO gas sensor have been reported using the electrochemical technique, namely, amperometric sensors [12-19] and potentiometric sensors [20-25]. In general, the potentiometric NO gas sensors are operated at higher temperature than that of the amperometric type. In the case of amperometric NO sensors, two electroanalytical methods have been employed for the detection of NO gas. One is mostly based on electrochemical oxidation [12-17], with only a few based on electrochemical reductions [18-19]. Table 2 summarizes the operating condition (e.g., potential and/or temperature) and output signal of the NO concentration studied in the gas phase at various sensing electrodes.

Chand [12] reported that NO electrooxidation occurred between 0.96 V and 1.03 V (vs. SHE) at a metal/membrane electrode with an acidic electrolyte. Sedlak and Blurton [13-16] also oxidized NO at 1.5, 1.6, and 0.9~1.5 V (vs. SHE) on Au/Teflon®, Au/hydrophobic plastic, and Au/C electrodes, respectively. They obtained a current plateau when potential was larger than 1.2 V (vs. SHE) [13]. The reported current density was 7.8 μA/cm² at a Au electrode. According to Jacquinot et. al. [17], NO could be oxidized at Pt/Nafion® and Au/Nafion® electrodes at 0.70 V vs. MSE (mercury-mercurous sulfate electrode) using 10 M H₂SO₄ electrolyte solution passing 0-1 ppm NO. The sensitivities of NO₂ and NO gases were 550 nA/ppm (or 696 nA/ppm/cm²) and 203 nA/ppm (or 257 nA/ppm/cm²), respectively, at the same Pt Nafion® electrode. The cross sensitivity of NO₂ with respect to NO was found to be 2.7. This NO gas sensor was significantly affected by interfering NO₂ gas in the 0-1 ppm range.

Table 1. The amperometric operating condition, concentration range, and detection limit for NO sensing studied in the solution phase at various sensing electrodes.

Sensing Electrodes	Operating Condition	NO conc. range	Detection Limit	Ref.
Pt/Nafion®	0.9 V vs. SSCE ^d	ca. 80~ 480 μM	N. A.	[1]
Pt/Nafion®/cellulose acetate	0.9 V vs. SSCE ^d	N. A.	N. A.	[1]
Pt/Nafion®	0.86 V vs. Ag/AgCl/sat. CuCl ^e	0~0.4 μM	N.A.	[2]
Pt/Ir	0.4~0.8 V vs. C	0.2 nM~1 μM	N. A.	[3]
Pt/Poly (4,4'-DHB) ^a	0.8 V vs. Ag/AgCl ^f	ca. 0~4.5 μM	40 nM	[4]
C/NiP/Nafion® ^b	0.63 V vs. SCE	ca.0~40 μM	1.5 nM	[5]
C/NiP/Nafion® ^b	0.64 V vs. SCE	0~300 μM	10 μM	[6]
C/Nafion®	0.86 V vs. Ag/AgCl/sat. CuCl ^e	0~1 μM	N. A.	[2]
C/Nafion® (D= 0.1 μm)	0.86 V vs. Ag/AgCl/sat. CuCl ^e	50 nM~1 mM	3 nM	[7]
C/Nafion® (D= 7 μm)	0.86 V vs. Ag/AgCl/sat. CuCl ^e	10 nM~5 μM	5 nM	[8]
C/Nafion®	0.86 V vs. Ag/AgC/sat. CuCl ^e	0~0.4 μM	N. A.	[9]
C/silicon	0.86 V vs. Ag/AgCl/sat. CuCl ^e	0~100 μM	0.3 nM	[10]
M(salen)/Nafion® ^c	DPA ^g	ca. 19.6 nM~2.8 μM	ca. 10~20 nM	[11]

^a: 4,4'-DHB: 4,4'-dihydroxybenzophenone. ^b: NiP : Tetrakis (3-methoxy-4-hydroxyphenyl) nickel(II) porphyrin. ^c: M(salen): metal ethylenebis (salicylideneiminate); M= Co, Fe, Cu, Mn. ^d: SSCE: sodium chloride saturated calomel electrode (SCE). ^e: A saturated CuCl concentration is about 2.4 mM. ^f: The concentration of Cl⁻ was not reported. ^g: DPA: differential pulse amperometry. The sensors were cleaned at 0.50 V (vs. Ag/AgCl/sat. KCl solution) for 1s, then the potential was pulsed to 0.70 V for 50 ms and pulsed to 0.80 V for 50 ms. N. A.: not available

The main electrochemical oxidation of NO gas at the Au and Pt or its composite electrodes [12-17] involves transfer of three electrons and can be expressed as



Another high-temperature ($>300^{\circ}\text{C}$) electrochemical oxidation involves two-electron transfer. In this case, the oxidation reaction occurs at the Pt/CdCr₂O₄ [18], Au/pyrochlore-type oxide [22], Au/Pb₂Ru_{1.9}V_{0.1}O_{7-z} [23], Pt/CdMn₂O₄ [24], and Pt/Zr₂O [25] sensing electrodes can be written as



Table 2. The operating condition and output signal for NO sensing concentration studied in the gas phase at various electrodes.

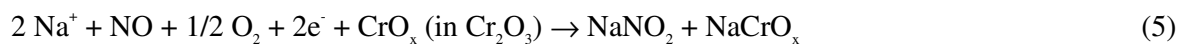
Sensing Electrodes	Operating Condition	Output Signal	Ref.
Noble metal/membrane ^a	0.96~1.03 V vs. SHE	Current	[12]
Au/Teflon [®]	1.5 V vs. SHE	Current	[13]
Au/hydrophobic plastic ^b	1.6 V vs. SHE	Current	[14, 15]
Au/C	0.9~1.5 V vs. SHE	Current	[16]
Au/Nafion [®]	0.7 V vs. MSE ^d	Current	[17]
Pt/Nafion [®]	0.7 V vs. MSE ^d	Current	[17]
Pt/Nafion [®]	1.15 V vs. sat. Ag/AgCl	Current	This work
Pt/CdCr ₂ O ₄	0.1 V vs. Pt (500 °C)	Current	[18]
Pt/Zr ₂ O	-0.55 V vs. C (e.g. 650 °C)	Current	[19]
NaNO ₂ /Au	150 °C	Potential	[20]
Cr ₂ O ₃ /Nasicon	250 °C	Potential	[21]
Au/pyrochlore-type oxide ^c	400 °C	Potential	[22]
Au/Pb ₂ Ru _{1.9} V _{0.1} O _{7-z}	400 °C	Potential	[23]
Pt/CdMn ₂ O ₄	600 °C	Potential	[24]
Pt/Zr ₂ O	300~400 °C	Potential	[25]

^a: Sensing material is mainly Au/Teflon[®]. Noble metal: e. g., Pt, Pd, Ir, and the like; Membrane: e. g., polyethylene (PE), polypropylene (PP), and the like. ^b: Sensing material is mainly Au/Teflon[®]. Hydrophobic plastic: e. g., polyacrylonitrile, polyvinyl chloride, polyvinyl alcohol, and carboxymethyl cellulose, or the like. ^c: Pyrochlore-type oxide: e.g., Pb₂[Ru_{2-x}Pb_x]O_{7-y} (x = 0-0.75) ; Pb₂Ir₂O_{7-y}. ^d: A saturated mercury-mercurous sulfate electrode (MSE, E = 0.64 V vs. SHE).

The electrochemical reduction at the Pt/Zr₂O electrode [19] involves transfer of two electrons and can be expressed as



The electrochemical reductions at the NaNO₂/Au [20] and Cr₂O₃/Nasicon [21] electrodes are assumed to involve transfer of one or two electrons, respectively. That is



It is well known that NO can be oxidized at a Au or its composite electrode. However, both the electrooxidation of NO and its amperometric responses on the Pt/Nafion® electrode are less studied. A Pt/Nafion® electrode repetitive potential scanning procedure was adopted to ensure the cleanliness of the electrode/electrolyte interface. By properly activating the Pt/Nafion® electrode, the electrooxidation of NO gas was carried out under potentiostatic conditions and the data were analyzed to obtain the kinetic parameters. According to Jacquinot et. al. [17], the NO sensor was significantly affected by interfering NO₂ gas at the Pt/Nafion® electrode. We therefore aimed in this study to increase the sensitivity of NO sensor and to decrease the NO₂ interference by adopting a proper activating procedure for the Pt/Nafion® electrode. The sensing characteristics of NO oxidation at the Pt/Nafion® interface, including the operating potential, sensitivity, and interfering gases (NO₂ and CO), were studied in the high concentration range of 0–500 ppm.

Experimental

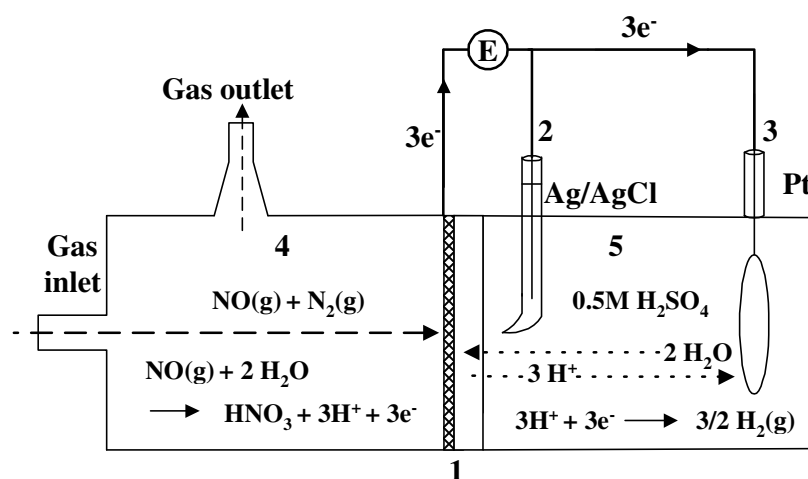
Sensing electrode characterization and experimental setup

The Pt/Nafion® electrode was prepared by the impregnation-reduction procedure. The platinum loading was controlled at 2 mg/cm². Details on the preparation of the Pt/Nafion® electrode, as well as the configuration of the sensor system, have been described previously [26]. N₂ (99.9995 %), standard NO gas (500 ppm) in N₂, standard NO₂ gas (541 ppm) in N₂, and standard CO gas (513 ppm) in N₂, were purchased from a local gas company (San-Fu Gas Co., Hsin-Chu). All chemicals used in this work were reagent grade and were used as received. Deionized water (DIW) was used throughout this work. All electrochemical measurements were performed at room temperature in a three-electrode configuration cell, with a Ag/AgCl/sat. KCl as the reference electrode. An EG&G (Model 273A) potentiostat/galvanostat was used to control the potential applied to the working electrode. The geometric area of the sensing electrode was 3.14 cm². The gas flow rate was controlled by a mass-flow-meter controller (Protec PC-540). The Sierra Instruments' Model 840 Side-Trak™ mass flow meters were used for precise measurement and control of process gases in different ranges from 0 to 500

ml/min. The gas flow rate was controlled at 200 ml/min in all experiments. Figure 1 is a schematic for the electrochemical oxidation of NO gas on the Pt/Nafion® electrode. The sensor consists of 5 components which include (1) working electrode (WE), (2) reference electrode (RE), (3) counter electrode (CE), (4) gas chamber, and (5) liquid chamber.

Pretreating or cleansing Pt/Nafion® electrode by cyclic voltammetric (CV) activation

Many researchers investigated Pt or Pt/Nafion® electrode for different applications. For example, Bilmes et. al. [27] studied the electrocatalytic oxidation of CO using polycrystalline Pt electrodes. Polycrystalline Pt electrodes were pretreated in 1 M HClO₄ by repetitive CV scanning at 10 V/s in the -0.02~1.35 V (vs. NHE) range to avoid the adsorption of CO on the Pt electrode surface. Parthasarathy et. al. [28-29] and Basura et. al. [30] found that the repeated potential scannings between the potentials of 0.05~1.50 V (vs. NHE) and of 0.25~1.50 V (vs. NHE), respectively, at a scan rate of 0.1 V/s were required to clean the Pt/Nafion® interface of residual impurities. To maintain the electrode/electrolyte interface in an activated state, the Pt/Nafion® (sensing) electrode used in this study was activated by repeated potential cycling for the purpose of cleansing. This was done in a cell containing 0.5 M H₂SO₄ by scanning the electrode potentials between -0.2 and 1.4 V for 10 cycles at a scan rate of 20 mV/s under N₂ at a flow rate of 200 ml/min. The intention of the repetitive scanning was to clean or remove adsorbed gases (NO, NO₂ or CO) by passing N₂. In fact, the open-circuit potential can be used as an indicator for the cleanliness of the electrode/electrolyte interface. Right after the cleaning, additional 30 min. to one hour was needed for the electrode to reach a steady-state open-circuit potential, or the equilibrium potential. The open-circuit potential was measured immediately after the activation procedure. The whole cleaning process thus can be followed by monitoring the drift of the open-circuit potential. Except for the fresh electrode, the experimental data reported below with Pt/Nafion® electrodes were all pretreated before each sensing experiment.



1. WE: Pt/Nafion® 2. RE: Ag/AgCl/sat'd KCl 3. CE: Pt disk 4. Gas chamber: NO(g) in N₂(g) or pure N₂(g) 5. Liquid chamber: 0.5 M H₂SO₄

Figure 1. An experimental setup for the electrochemical oxidation of NO at a Pt/Nafion® electrode.

Results and Discussion

Real surface area of a fresh Pt/Nafion® electrode

Typical cyclic voltammogram (CV) of the fresh Pt/Nafion® electrode, in contact with 0.5 M H₂SO₄ solution in N₂ atmosphere at a flow rate of 200 ml/min, is shown in Fig. 2. The potential was scanned from -0.2 to 1.4 V at a scan rate of 20 mV/s. The peaks are designated in their order of appearance with increasing anodic potential as “O_{A1}”, “O_{A2}”, and “O_{A3}”, continuing into O₂ evolution process. H adsorption and ionization peaks “H_A”, “H_c”, etc. at more cathodic potentials are also indicated together with the cathodic region “O_C” for surface oxide reduction.

The cathodic and anodic peaks at E < 0.2 V (vs. Ag/AgCl/sat'd KCl) are respectively due to the electrochemical adsorption and desorption of hydrogen on the Pt/Nafion® electrode. The anodic peaks at E > 0.6 V are ascribed to the surface oxide formation and the cathodic peak at E ≈ 0.43 V is ascribed to the surface oxide reduction. The evolutions of hydrogen and oxygen take place at about E < -0.2 V and E > 1.25 V, respectively. The electrochemical active surface area of platinum was determined from integration of the charge of oxidation of the adsorbed hydrogen region of the stationary CV after subtracting the double layer charge and use 210 μC/real cm² as the saturation coverage [31-34]. The value of Area I, charge of desorbed hydrogen, in Fig. 2 was measured to be 8.10 mC/cm², hence the roughness factor (real area/geometric area) for the Pt/Nafion® electrode would be 38.6 real cm²/cm² of the geometrical area. This value is reasonable, as compared to the value reported in the literature [35], considering the small amount of Pt loading (2 mg/cm²) used in this study.

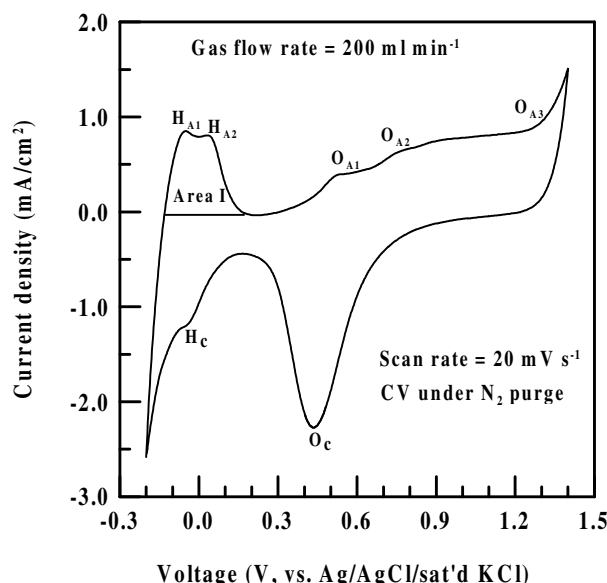


Figure 2. Typical cyclic voltammogram (CV or the potentiodynamic current-potential profile) for a Pt/Nafion® electrode run in pure N₂ at 20 mV/sec. Solution phase: 0.5 M H₂SO₄; The gas flow rate is maintained at 200 ml/min.

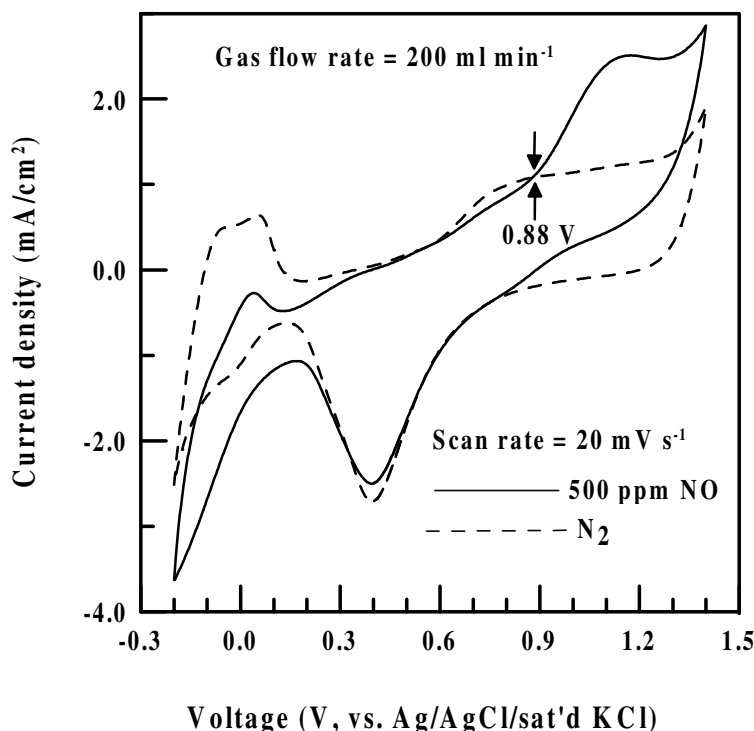
CV of a Pt/Nafion® electrode in N₂ and NO

Figure 3. Typical CVs for a Pt/Nafion® electrode run at 20 mV/sec. Gas phase: (—) 500 ppm NO; (---) pure N₂. Solution phase: 0.5 M H₂SO₄; The gas flow rate is maintained at 200 ml/min.

The typical CVs of a Pt/Nafion® electrode in contact with 0.5 M H₂SO₄ solution, in the presence of N₂ (dotted line) and 500 ppm NO (solid line) gases, are shown in Fig. 3. The results were obtained by the CV activation procedure as detailed in the experimental section. The peak potential for reduction of platinum oxides ($E_{p,c}$) was found at approximately 0.4 V in N₂. The anodic current density increased in the range at 0.88~1.15 V due to the NO oxidation when 500 ppm NO was applied. The onset potential for NO oxidation occurring at the Pt surface was found at 0.88 V. The peak potential for NO oxidation ($E_{p,a}$) at the Pt/Nafion® electrode was found approximately at 1.15 V. The peak potential for reduction of platinum oxides was found also at 0.4 V in the presence of 500 ppm NO. However, the area of CV in NO was smaller than that of CV in N₂ at the potential range between -0.2 and 0.15 V. This is due to the NO adsorption which retarded the H₂ adsorption at surface of the Pt/Nafion® electrode.

Effect of sensing potential-Polarization data

The steady-state polarization data, or the net current density (i) vs. potential (E) plot for the oxidation of 500 ppm NO at the Pt/Nafion® electrode, are shown in Figure 4. At each potential level, the procedure began with stepping the potential from the open-circuit potential to the chosen potential under 500 ppm NO in N₂, followed by a CV activation process.

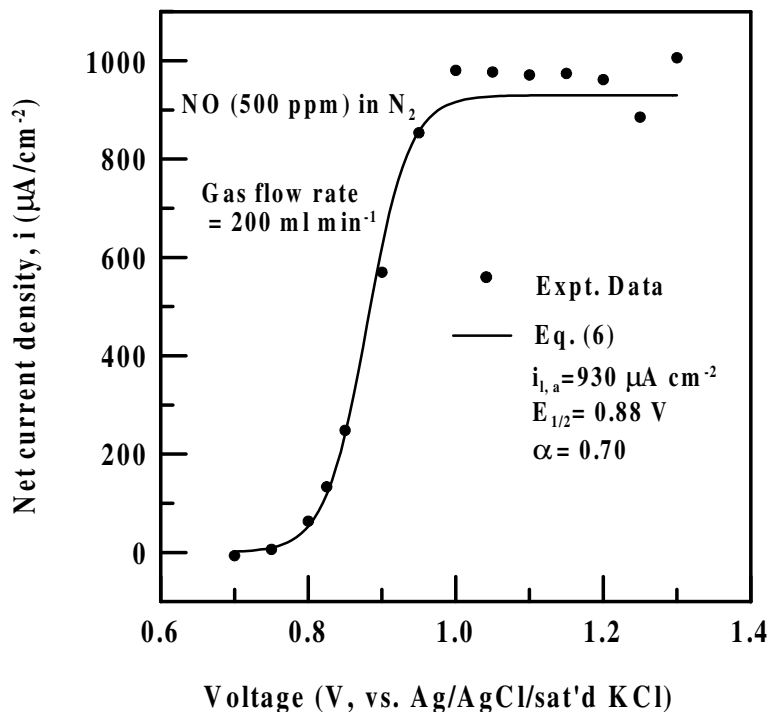


Figure 4. The net current density-potential (i - E) data for oxidizing 500 ppm NO at a Pt/Nafion[®] electrode. The gas flow rate is maintained at 200 ml/min. The solid curve is obtained by plotting Eq. (6) with appropriate parameters.

Then a background current density at the same potential level was obtained in N_2 purge. Finally, this run was ended with a final CV activation. The complete polarization data were obtained by repeating the procedure mentioned above. The potential of the Pt/Nafion[®] electrode was increased sequentially from 0.7 to 1.3 V. The net current density increased from 6.4 to $980 \mu\text{A}/\text{cm}^2$ as the operating potential was increased from 0.75 to 1.0 V. The zero net current density was experimentally observed at 0.744 V, which corresponds to the equilibrium potential for the oxidation reaction, E_{eq} . For the NO oxidation reaction taking place in the kinetic controlled region, the potential at the Pt/Nafion[®] electrode should be controlled between 0.75 and 0.85 V; while to ensure the operation in the diffusive or mass transfer controlled region, the Pt/Nafion[®] electrode is preferably operated in the potential range of 1.0 to 1.2 V. In fact, the polarization data over a wide potential range, including both kinetic and mass transfer controlled regions, can be expressed by the following transcendental equation [36]

$$\frac{i}{i_{l,a}} = \frac{1}{1 + e^{-(1-\alpha)nF(E-E_{1/2})/RT}} \quad (6)$$

where $i_{l,a}$, α , n , and F are the anodic limiting current density, the charge transfer coefficient, the stoichiometric number of electrons involved in the electrode reaction, and Faraday's constant, respectively. R and T have their usual meaning. $E_{1/2}$ is called the half-wave potential; that is, $E=E_{1/2}$ when $i=i_{l,a}/2$.

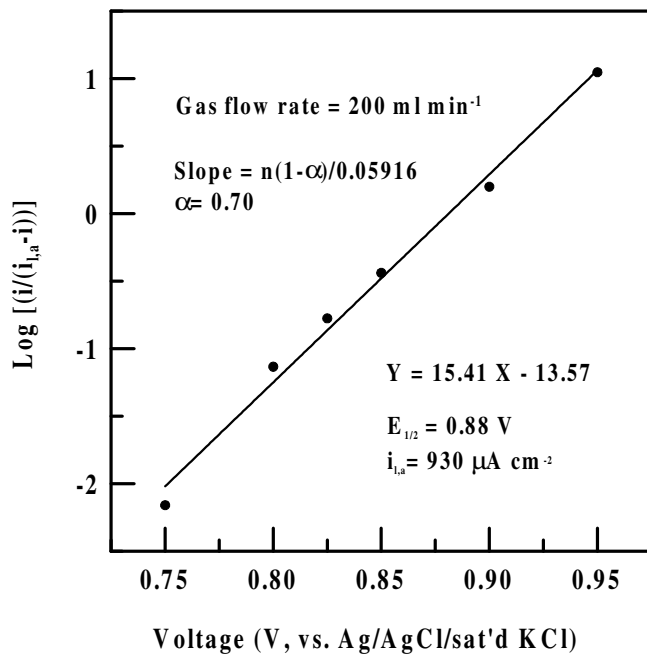


Figure 5. A plot of $\log [i/(i_{l,a}-i)]$ vs. E , from which the value of α can be obtained from the slope and the value of $E_{1/2}$ from the intercept.

The smooth curve in Figure 4 is obtained by plotting Eq. (6) with $i_{l,a}=930 \mu\text{A}/\text{cm}^2$, $E_{1/2}=0.88 \text{ V}$, and $\alpha=0.70$. In fact, when an electrochemical reaction conforms to Eq. (6), a plot of $\log [i/(i_{l,a}-i)]$ vs. E is a straight line with a slope of $(1-\alpha)nF/2.3RT$ (or $n(1-\alpha)/0.05916 \text{ V}^{-1}$ at 25°C) and has an E -intercept of $E_{1/2}$. This is shown in Fig. 5. The obtained value of $E_{1/2}(0.88 \text{ V})$ from the intercept is the same as the onset potential (0.88 V) obtained earlier for NO oxidation under the same experimental conditions, as judged by the CVs in Figure 3.

Tafel kinetics

It would be interesting to extract the kinetic parameters for the NO oxidation. This can be done by plotting $\log [i]$ vs. η , known as a Tafel plot. For sufficiently large values of overpotential applied ($\eta \equiv E-E_{eq}>118 \text{ mV}/n=118/3 \approx 40 \text{ mV}$), the overpotential η can be expressed as [36]

$$\eta = \frac{2.303RT}{(1-\alpha)nF} \log\left(\frac{i}{i_0}\right) \quad (7)$$

where i_0 is the exchange current density for the electrochemical reaction. A plot of $\log [i]$ vs. η is shown in Fig. 6, from which α can be obtained from the slope and i_0 from the intercept.

The experimental value of $E_{eq}=0.744 \text{ V}$ is used here to obtain the values of the overpotential. The obtained values of α and i_0 are 0.77 and $14 \mu\text{A}/\text{cm}^2$, respectively. Thus, the overpotential can be expressed by the empirical equation $\eta = a + b \log [i] = 0.41 + 0.08 \log [i]$. This approach has the advantage of being applicable to an electrode reaction that has appreciable overpotentials but negligible

mass-transfer effects. The obtained α value of 0.77 in the kinetic controlled region ($E=0.80\sim0.85$ V) is more reliable than that of 0.70, which was obtained earlier from a wide potential range ($E=0.70\sim1.30$ V). As the value of the charge transfer coefficient (α) deviates from 0.5, this implies that the energy barrier for the electrooxidation of NO at the Pt/Nafion® electrode is unsymmetrical. In addition, the kinetics for the electrooxidation is facile due to its large exchange current density ($i_0 = 14 \mu\text{A}/\text{cm}^2$).

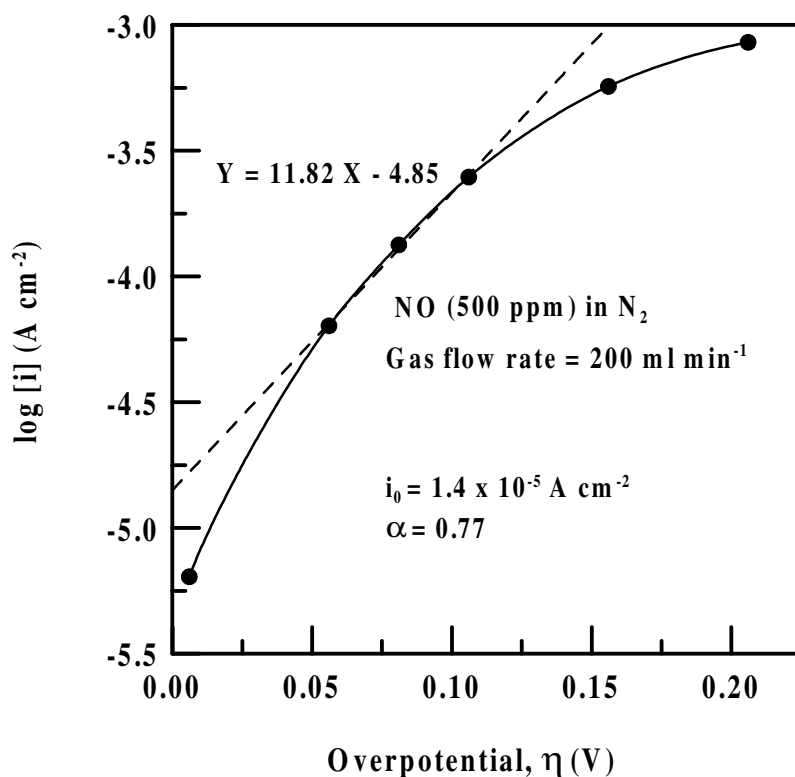


Figure 6. A plot of $\log [i]$ vs. overpotential in the kinetic controlled region. The slope gives the value of α and the intercept gives the value of i_0 .

Interferences and sensitivities

Interfering species, like nitrogen dioxide (NO_2) and carbon monoxide (CO), usually coexist with NO in the measuring atmospheres. It is, therefore, necessary to test both NO_2 and CO for the effects of interference and cross sensitivity. The cross sensitivity, or the sensitivity ratio, is defined as the ratio of the sensitivity for an interfering species with respect to the sensitivity for NO oxidation under the same applied potential and the same gas flow rate. Figure 7 shows the net current densities vs. concentrations of NO, NO_2 , and CO in the range from 0 to 500 ppm at the same Pt/Nafion® sensing electrode.

The anodic polarization was carried out at an applied potential of 1.15 V and a fixed flow rate of 200 ml/min. When passing NO, NO_2 , and CO, the sensing responses were linear for all three gases in the concentration range 0–500 ppm. According to Fig. 7, the sensitivities (0–500 ppm) were calculated to be $1.86 \mu\text{A}/\text{ppm}/\text{cm}^2$, $0.1 \mu\text{A}/\text{ppm}/\text{cm}^2$, and $0 \mu\text{A}/\text{ppm}/\text{cm}^2$ at the same Pt/Nafion® electrode for NO,

NO_2 and CO, respectively. The sensitivity ($1.86 \mu\text{A}/\text{ppm}/\text{cm}^2$) was 7 times higher than that ($0.26 \mu\text{A}/\text{ppm}/\text{cm}^2$) of Jacquinot et. al. [17] at the Pt/Nafion® electrode for NO sensing. The cross sensitivities (sensitivity of interfering gas/sensitivity of NO) for NO_2 and CO in the 0-500 ppm range

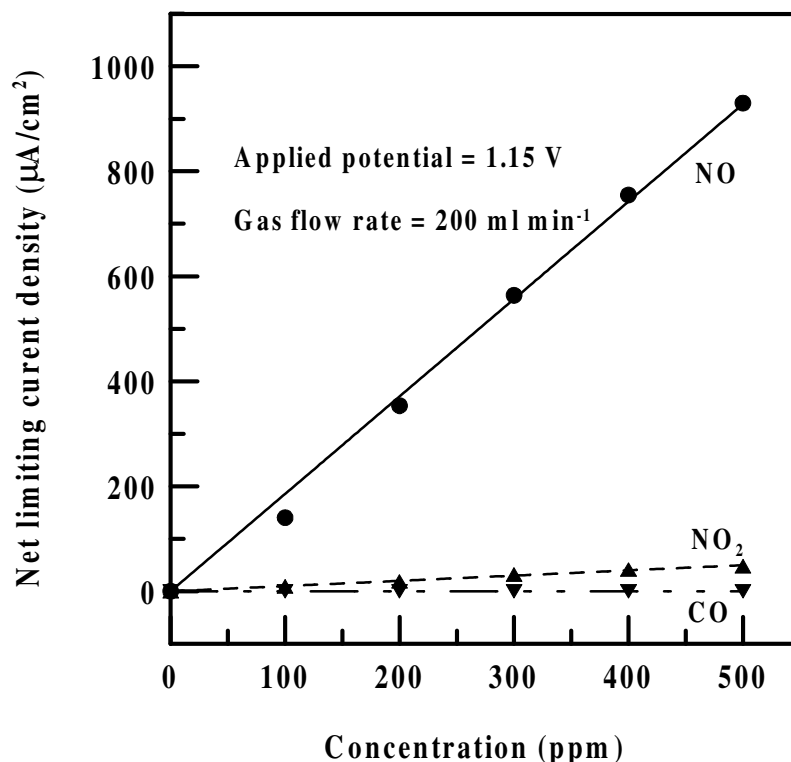


Figure 7. The net limiting current density dependence of NO, NO_2 , and CO concentrations (0-500 ppm) at the same sensing electrode.

were found to be around 0.05 and 0, respectively. Therefore, this sensor was only slightly affected by NO_2 gas, but was hardly affected by CO gas. Thus, the cross sensitivities found in this study in the range 0-500 ppm was smaller than those reported in the literature in the range 0-1 ppm [17]. One of the reasons may have to do with the pretreatment procedure for the electrode, i.e., the repetitive scanning that was so pretreated on the electrode may increase the active sites for NO reaction. When compared with the literature, another possibility is that different morphological platinum oxide surfaces may exist and cause different mechanisms for electrooxidation of NO gas. Although it is possible that the morphological difference of the electrode may play a role, it is very likely that the CV activation procedure plays a crucial role in enhancing both sensitivity and selectivity.

In general, the differences in selectivity of NO over NO_2 might also, besides activation, be related to the applied potential. However, according to our previous study [26], the variation of the applied potential has no effect on the current response for sensing NO_2 at the Pt/Nafion® electrode as long as the electrode is operated in the diffusive region (0.95 to 1.15 V).

Conclusion

This work reported on the electrooxidation of NO gas at the Pt/Nafion® electrode and on the amperometric NO sensing based on the same electrode. To study the electrooxidation reaction of NO on the Pt/Nafion® electrode, the experimental data were compared with a transcendental equation, from which the half-wave potential of the reaction was found to be 0.88 V (vs. Ag/AgCl/sat'd KCl). The current densities collected in the kinetic region follows the Tafel kinetics, from which the kinetic parameters for the reaction were extracted. The obtained charge transfer coefficient (α) and the exchange current density (i_0) were 0.77 and 14 $\mu\text{A}/\text{cm}^2$, respectively. For sensor application, the potential of the Pt/Nafion® electrode was chosen in the diffusive region (or mass transfer controlled region) of preferably 1.15 V (vs. Ag/AgCl/sat'd KCl). The sensitivity was found to be 1.86 $\mu\text{A}/\text{ppm}/\text{cm}^2$ for a fixed flow rate of 200 ml/min. The sensitivity was 7 times higher than that reported in literature. Presumably, this is due to the CV activation that increases the active sites for NO oxidation. The cross sensitivities of NO₂ and CO were found to be 0.05 and 0, respectively.

Acknowledgement

This research was supported by the Program for Promoting Academic Excellence of Universities, sponsored by the Ministry of Education of the Republic of China, under grant number EX-91-E-FA09-5-4.

References

1. Pariente, F.; Alonso, J. L.; Abruna, H. D. *J. Electroanal. Chem.* **1994**, 379, 191-197.
2. Zhang, X.; Cardosa, L.; Broderick, M.; Fein, H.; Davies, I.R. *Electroanalysis* **2000**, 12, 425-428.
3. Ichimori, K.; Ishida, H.; Fukahori, M.; Nakazawa, H.; Murakami, E. *Rev. Sci. Instrum.* **1994**, 65, 2714-2718.
4. Pallini, M.; Curulli, A.; Amine, A.; Palleschi, G. *Electroanalysis* **1998**, 10, 1010-1016.
5. Lantoine, F.; Trevin, S.; Bedioui, F.; Devynck, J. *J. Electroanal. Chem.* **1995**, 392, 85-89.
6. Malinski, T.; Taha, Z. *Nature* **1992**, 358, 676-679.
7. Zhang, X.; Kislyak, Y.; Cardosa, L.; Broderick, M.; Fein, H. *Free Radic. Biol. Med.* **2000**, 29, S78.
8. Zhang, X.; Cardosa, L.; Broderick, M.; Fein, H.; Lin, J. *Electroanalysis* **2000**, 12, 1113-1117.
9. Zhang, X.; Broderick, M. *Mod. Asp. Immunobiol.* **2000**, 1, 160-165.
10. Zhang, X.; Lin, J.; Cardosa, L.; Broderick, M.; Darley-Usmar, V. *Electroanalysis* **2002**, 14, 697-703.
11. Mao, L.; Yamamoto, K.; Zhou, W.; Jin, L. *Electroanalysis*, **2000**, 12, 72-77.
12. Chand, R. U.S. Patent No. **1971**, 3,622,487.
13. Sedlak, J. M.; Blurton, K. F. *J. Electrochem. Soc.* **1976**, 123, 1476-1478.

14. Blurton, K.F.; Sedlak, J. M. *U.S. Patent No. 1977*, 4,001,103.
15. Blurton K. F.; Sedlak, J. M. *U.S. Patent No. 1977*, 4,052,268.
16. Blurton K. F.; Sedlak, J. M. *U.S. Patent No. 1977*, 4,042,464.
17. Jacquinot, P.; Hodgson, A. W. E.; Hauser, P. C. *Anal. Chim. Acta* **2001**, 443, 53-61.
18. Miura, N.; Lu, G.; Yamazeo, N. *Sens. Actuators B* **1998**, 52, 169-178.
19. Somov, S.; Reinhardt, G.; Guth, U.; Gopel, W. *Sens. Actuators B* **1996**, 35-36, 409-418.
20. Yao, S.; Shimizu, Y.; Miura, N.; Yamazoe, N. *Chem. Letter* **1992**, 587-590.
21. Shimizu Y.; Maeda, K. *Chem. Letter* **1996**, 117-118.
22. Shimizu, Y.; Maeda, K. *Sens. Actuators B* **1998**, 52, 84-89.
23. Shimizu, Y.; Nishi, H.; Suzuki, H.; Maeda, K. *Sens. Actuators B* **2000**, 65, 141-143.
24. Morio, N.; Kurosawa, H.; Hasei, M.; Lu, G.; Yamazoe, N. *Solid State Ionics* **1996**, 86-88, 1069-1073.
25. Takashi, O.; Masaharu, H.; Akira, K. *EP Patent No. 2002*, 1,167,957.
26. Ho, K. C.; Hung, W. T. *Sens. Actuators B* **2001**, 79, 11-16.
27. Bilmes, S. A.; De Tacconi, N. R.; Arvia, A. J. *J. Electroanal. Chem.* **1984**, 164, 129-143.
28. Parthasarathy, A.; Srinivasan, S.; Appleby, A. J.; Martin, C. R. *J. Electrochem. Soc.* **1992**, 139, 2530-2537.
29. Parthasarathy, A.; Dave, B.; Srinivasan, S.; Appleby, A. J.; Martin, C. R. *J. Electrochem. Soc.* **1992**, 139, 1634-1641.
30. Basura, I.; Beattie, P. D.; Holcroft, S. *J. Electroanal. Chem.* **1998**, 458, 1-5.
31. Will, F. G. *J. Electrochem. Soc.* **1965**, 112, 451-455.
32. Biegler, T.; Rand, D. A. J.; Woods, R. *J. Electroanal. Chem.* **1971**, 29, 269-277.
33. Woods, R. *J. Electroanal. Chem. Interfacial Electrochem.* **1974**, 49, 217-226.
34. Angerstein-Kozlowska, H.; Conway, B. E.; Sharp, W. B. A. *J. Electroanal. Chem. Interfacial Electrochem.* **1973**, 43, 9-36.
35. Opekar, F.; Stulik, K. *Anal. Chim. Acta* **1999**, 385, 151-162.
36. Bard, A. J.; Faulkner, L. R. *Electrochemical Methods*; 2nd Ed.; John Wiley & Sons: New York, **2001**, Chapter 1 and 3.

Sample Availability: Available from the authors.